

Jupiter’s Dynamical Love Number

DONG LAI¹

¹*Cornell Center for Astrophysics and Planetary Science, Department of Astronomy, Cornell University, Ithaca, NY 14853*

Abstract

Recent observations by the *Juno* spacecraft have revealed that the tidal Love number k_2 of Jupiter is 4% lower than the hydrostatic value. We present a simple calculation of the dynamical Love number of Jupiter that explains the observed “anomaly”. The Love number is usually dominated by the response of the (rotation-modified) f-modes of the planet. Our method also allows for efficient computation of high-order dynamical Love numbers. While the inertial-mode contributions to the Love numbers are negligible, a sufficiently strong stratification in a large region of the planet’s interior would induce significant g-mode responses and influence the measured Love numbers.

Keywords: dynamical tides — giant planets — Jupiter’s interior — gravitational fields

1. INTRODUCTION

The *Juno* spacecraft recently found an “anomaly” in Jupiter’s tidal Love number: the measured $k_2 = 0.565 \pm 0.006$ (Durante et al. 2020) appears to be smaller than the theoretical hydrostatic value $k_2^{(\text{hs})} = 0.590$ (Wahl et al. 2020) by 4%. This discrepancy may be explained in terms of dynamical tides, i.e., Jupiter’s response to the finite-frequency tidal forcings from the Galilean moons (Idini & Stevenson 2021). Here we present a simple calculation that explains this Love number “anomaly” quantitatively. Naive expectation would suggest a $1/(\omega_\alpha^2 - \omega^2)$ enhancement (where ω_α is the f-mode frequency of the planet) of the tidal response due to the finite tidal frequency (ω) as compared to the hydrostatic ($\omega = 0$) response. The key to obtain the correct answer is to treat the rotational (Coriolis) effect on the modes of a rotating planet and their tidal responses in a self-consistent way. Our general method also allows for efficient computation of high-order dynamical Love numbers k_{lm} , as well as the inclusion of the contributions to k_{lm} from the inertial modes (due to planetary rotation) and g-modes (due to stable stratification in the planetary interior).

2. DYNAMICAL LOVE NUMBER AND NORMAL MODES

Consider a planet (mass M , radius R and spin angular frequency Ω_s) orbited by a satellite (mass M') in a circular orbit with semi-major axis a and orbital frequency Ω_{orb} . We assume the spin axis is aligned with the orbital axis. In the frame corotating with the planet, the (lm) -component of the tidal potential produced by M'

on the planet is

$$U(\mathbf{r}, t) = -A_{lm} r^l Y_{lm}(\theta, \phi) e^{-i\omega t}, \quad (1)$$

where $A_{lm} = (GM'/a^{l+1})W_{lm}$ (with W_{lm} a dimensionless constant; $W_{lm} \neq 0$ when $l + m = \text{even}$), $\mathbf{r} = (r, \theta, \phi)$ specifies the position vector (in spherical coordinates) measured from the center of the planet, and

$$\omega = m(\Omega_{\text{orb}} - \Omega_s) \quad (2)$$

is the tidal forcing frequency. It suffices to consider only $m > 0$. The relevant non-zero tidal components are $(lm) = (2, 2), (3, 1), (3, 3), (4, 2), (4, 4)$ etc.

The linear response of the planet to the tidal forcing is specified by the Lagrangian displacement, $\xi(\mathbf{r}, t)$, of a fluid element from its unperturbed position. In the rotating frame of the planet, the equation of motion takes the form

$$\frac{\partial^2 \xi}{\partial t^2} + 2\Omega_s \times \frac{\partial \xi}{\partial t} + \mathbf{C} \cdot \xi = -\nabla U, \quad (3)$$

where \mathbf{C} is a self-adjoint operator (a function of the pressure and gravity) acting on ξ (see, e.g., Friedman & Schutz 1978). A free mode of frequency ω_α (in the rotating frame) with $\xi_\alpha(\mathbf{r}, t) = \xi_\alpha(\mathbf{r}) e^{-i\omega_\alpha t} \propto e^{im\phi - i\omega_\alpha t}$ satisfies

$$-\omega_\alpha^2 \xi_\alpha - 2i\omega_\alpha \Omega_s \times \xi_\alpha + \mathbf{C} \cdot \xi_\alpha = 0, \quad (4)$$

where $\{\alpha\}$ denotes the mode index, which includes the azimuthal number m . We carry out phase-space mode expansion (Schenk et al. 2002)

$$\begin{bmatrix} \xi \\ \partial \xi / \partial t \end{bmatrix} = \sum_\alpha c_\alpha(t) \begin{bmatrix} \xi_\alpha(\mathbf{r}) \\ -i\omega_\alpha \xi_\alpha(\mathbf{r}) \end{bmatrix}. \quad (5)$$

Using the orthogonality relation $\langle \boldsymbol{\xi}_\alpha, 2i\boldsymbol{\Omega}_s \times \boldsymbol{\xi}_{\alpha'} \rangle + (\omega_\alpha + \omega_{\alpha'})\langle \boldsymbol{\xi}_\alpha, \boldsymbol{\xi}_{\alpha'} \rangle = 0$ (for $\alpha \neq \alpha'$), where $\langle A, B \rangle \equiv \int d^3x \rho (A^* \cdot B)$, we find (Lai & Wu 2005)

$$\dot{c}_\alpha + i\omega_\alpha c_\alpha = \frac{iQ_{\alpha,lm}}{2\varepsilon_\alpha} A_{lm} e^{-i\omega t}, \quad (6)$$

where

$$Q_{\alpha,lm} \equiv \langle \boldsymbol{\xi}_\alpha, \nabla(r^l Y_{lm}) \rangle = \int d^3x r^l Y_{lm} \delta\rho_\alpha^*, \quad (7)$$

$$\varepsilon_\alpha \equiv \omega_\alpha + \langle \boldsymbol{\xi}_\alpha, i\boldsymbol{\Omega}_s \times \boldsymbol{\xi}_\alpha \rangle, \quad (8)$$

and we have used the normalization $\langle \boldsymbol{\xi}_\alpha, \boldsymbol{\xi}_\alpha \rangle = 1$. In Eq. (7), $\delta\rho_\alpha$ is the Eulerian density perturbation associated with the eigenfunction $\boldsymbol{\xi}_\alpha$.

Equation (6) has stationary solution

$$c_\alpha(t) = \frac{Q_{\alpha,lm}}{2\varepsilon_\alpha(\omega_\alpha - \omega)} A_{lm} e^{-i\omega t}. \quad (9)$$

The gravitational perturbation associated with the density perturbation $\delta\rho(\mathbf{r}, t) = \sum_\alpha c_\alpha(t) \delta\rho_\alpha(\mathbf{r})$, evaluated at the planet's surface ($r = R$), is

$$\delta\Phi(\mathbf{r}, t) \Big|_{r=R} = - \sum_\alpha c_\alpha(t) \frac{4\pi}{2l+1} \frac{GMQ_{\alpha,lm}}{R} Y_{lm}. \quad (10)$$

Thus the tidal Love number is

$$k_{lm} = \frac{\delta\Phi}{U} \Big|_{r=R} = \frac{2\pi}{2l+1} \sum_\alpha \frac{\bar{Q}_{\alpha,lm}^2}{\bar{\varepsilon}_\alpha(\bar{\omega}_\alpha - \bar{\omega})}. \quad (11)$$

In the above equation, the tidal overlap coefficient $\bar{Q}_{\alpha,lm}$ and the mode frequencies $\bar{\omega}_\alpha$ and $\bar{\varepsilon}_\alpha$ are in units where $G = M = R = 1$, i.e., $\bar{\omega}_\alpha = \omega_\alpha/(GM/R^3)^{1/2}$, etc. Note that for a given $m > 0$, the sum in Eq. (11) includes modes with positive ω_α and negative ω_α , corresponding to prograde (with respect to the planet's rotation) and retrograde modes.

3. F-MODE CONTRIBUTION

In most situations, the sum in Eq. (11) is dominated by f-modes since they have the largest tidal overlap $Q_{\alpha,lm}$. For planetary rotation rate Ω_s much less than the breakup rate $(GM/R^3)^{1/2}$, (e.g., $\bar{\Omega}_s = 0.288$ for Jupiter), the effect of rotation on the modes can be treated perturbatively (e.g. Unno et al. 1989). Let ω_0 (> 0) be the mode frequency of a non-rotating planet, then for a given $m > 0$, the sum in Eq. (11) includes

$$\varepsilon_\alpha \simeq \pm\omega_0, \quad (12)$$

$$\omega_\alpha = \pm\omega_0 - mC\Omega_s, \quad (13)$$

with

$$\begin{aligned} mC &\equiv \int d^3x \rho \boldsymbol{\xi}_{\alpha,0}^* \cdot (i\hat{\mathbf{z}} \times \boldsymbol{\xi}_{\alpha,0}) \\ &= m \int_0^R dr \rho r^2 (2\xi_r \xi_\perp + \xi_\perp^2), \end{aligned} \quad (14)$$

Table 1. Oscillation modes of non-rotating polytropic ($n = 1$) planet model

| | | ω_0 | Q_l | C |
|------------------|----|------------|-------------|------------|
| $\Gamma_1 = 2$ | | | | |
| $l = 2$ | f | 0.1227E+01 | 0.5579E+00 | 0.4991E+00 |
| | p1 | 0.3462E+01 | 0.2690E-01 | 0.1119E+00 |
| $l = 3$ | f | 0.1698E+01 | 0.5846E+00 | 0.3321E+00 |
| | p1 | 0.3975E+01 | 0.4054E-01 | 0.8627E-01 |
| $l = 4$ | f | 0.2037E+01 | 0.5979E+00 | 0.2489E+00 |
| | p1 | 0.4409E+01 | 0.4623E-01 | 0.6984E-01 |
| $\Gamma_1 = 2.1$ | | | | |
| $l = 2$ | f | 0.1228E+01 | 0.5580E+00 | 0.4989E+00 |
| | g1 | 0.2566E+00 | -0.3497E-02 | 0.7094E-01 |
| | g2 | 0.1770E+00 | 0.8364E-03 | 0.1193E+00 |
| | g3 | 0.1361E+00 | -0.2472E-03 | 0.1380E+00 |
| $l = 3$ | f | 0.1700E+01 | 0.5848E+00 | 0.3320E+00 |
| | g1 | 0.3081E+00 | -0.3260E-02 | 0.8812E-02 |
| | g2 | 0.2220E+00 | 0.8906E-03 | 0.4452E-01 |
| | g3 | 0.1750E+00 | -0.2839E-03 | 0.5904E-01 |
| $\Gamma_1 = 2.4$ | | | | |
| $l = 2$ | f | 0.1230E+01 | 0.5580E+00 | 0.4985E+00 |
| | g1 | 0.4688E+00 | -0.1313E-01 | 0.1057E+00 |
| | g2 | 0.3270E+00 | 0.3071E-02 | 0.1342E+00 |
| | g3 | 0.2526E+00 | -0.8961E-03 | 0.1464E+00 |
| $l = 3$ | f | 0.1703E+01 | 0.5850E+00 | 0.3317E+00 |
| | g1 | 0.5681E+00 | -0.1216E-01 | 0.3321E-01 |
| | g2 | 0.4117E+00 | 0.3257E-02 | 0.5622E-01 |
| | g3 | 0.3254E+00 | -0.1031E-02 | 0.6603E-01 |

NOTE— ω_0 and Q_l are the mode frequency and tidal overlap coefficient (Eq. 7), both in units such that $G = M = R = 1$, and C is defined in Eq. (14). The planet's density profile is that of $n = 1$ polytrope (with the equation of state $P \propto \rho^2$). Here Γ_1 is the adiabatic index. G-modes exit if $\Gamma_1 > \Gamma$ in some regions of the planet's interior. For the isentropic model ($\Gamma_1 = \Gamma = 2$), we list the properties for the f-mode and the first radial-order p-mode. For models with $\Gamma_1 > \Gamma$, we list the properties for the f-mode and the first three radial-order g-modes.

where $\boldsymbol{\xi}_{\alpha,0} = [\xi_r(r)\hat{\mathbf{r}} + \xi_\perp(r)r\nabla_\perp] Y_{lm}$ is the mode eigenvector of a non-rotating planet. To a good approximation, we can also set $Q_{\alpha,lm}$ to be the non-rotating value, i.e.,

$$Q_{\alpha,lm} \simeq Q_l. \quad (15)$$

Thus Eq. (11) reduces to

$$k_{lm} \simeq \left(\frac{4\pi}{2l+1} \right) \frac{\bar{Q}_l^2}{\bar{\omega}_0^2 - (mC\bar{\Omega}_s + \bar{\omega})^2}. \quad (16)$$

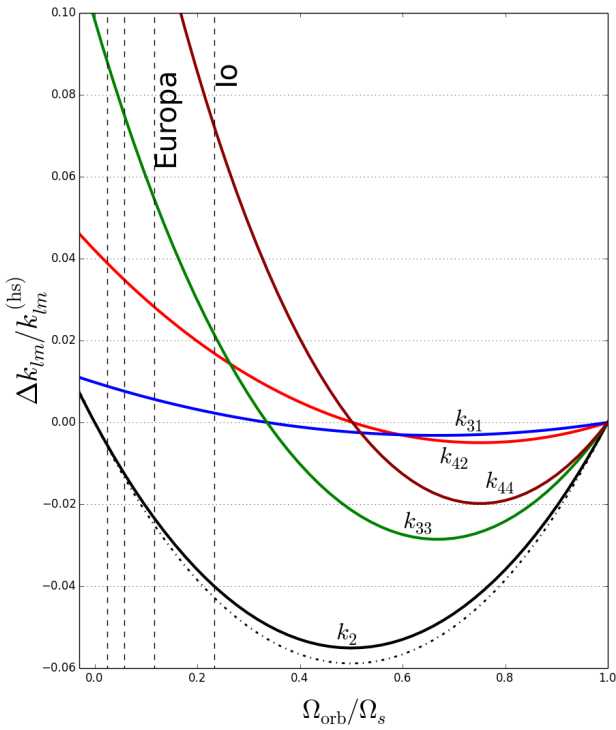


Figure 1. Dynamical correction $\Delta k_{lm}/k_{lm}^{(hs)} = (k_{lm} - k_{lm}^{(hs)})/k_{lm}^{(hs)}$ to Jupiter’s tidal Love number as a function of the orbital frequency Ω_{orb} of the perturbing satellite (in units of the spin frequency Ω_s). All results (solid curves) are computed using the $n = 1$ (isentropic) polytrope model, except that the dot-dashed curve is for $k_2 = k_{22}$ computed using the $n = 0.9$ polytrope model. The vertical dashed lines specify the orbital frequencies of Io, Europa, Ganymede and Callisto (from right to left). The -4% “anomaly” of k_2 observed by *Juno* can be explained by the planetary model with $n \simeq 1$.

For an incompressible planet model ($n = 0$ polytrope), the $l = 2$ mode (Kelvin mode) has

$$\bar{\omega}_0 = \frac{2}{\sqrt{5}}, \quad \bar{Q}_2 = \left(\frac{3}{2\pi} \right)^{1/2}, \quad C = \frac{1}{2}. \quad (17)$$

Thus

$$k_2 \equiv k_{22} \simeq \frac{3}{2} \left[1 - \frac{5}{4} (\bar{\Omega}_s + \bar{\omega})^2 \right]^{-1}, \quad (18)$$

with $\bar{\omega} = 2(\bar{\Omega}_{\text{orb}} - \bar{\Omega}_s)$.

Giant planets are approximately described by a $n = 1$ polytrope (corresponding to $P \propto \rho^2$). Table 1 lists the numerical values of ω_0 , Q_l and C for several non-rotating polytropic models (with different levels of stratification; see Section 5). For $l = m = 2$ tidal response (and $n = 1$), $2C \simeq 1$, we have

$$k_2 \simeq 0.520 \left[1 - 0.664 (\bar{\Omega}_s + \bar{\omega})^2 \right]^{-1}. \quad (19)$$

Applying to the Jupiter-Io system: Jupiter has $\bar{\Omega}_s = 0.288$ [with spin period 9.925 hrs and $2\pi(R^3/GM)^{1/2} = 2.863$ hrs], Io has $\bar{\Omega}_{\text{orb}} = 0.0674$ (orbital period 1.769 days), so $\bar{\omega} = -0.441$. Thus the hydrostatic and dynamical k_s values are

$$k_2^{(\text{hs})} = 0.550, \quad k_2 = 0.528 = 0.960 k_2^{(\text{hs})} \quad (20)$$

This explains the 4% discrepancy between k_2 and $k_2^{(\text{hs})}$. Note that our static $k_2^{(\text{hs})}$ does not agree with the value (0.590) from Wahl et al. (2020). This could arise for two reasons: (i) The simple $n = 1$ polytropic model does not precisely represent Jupiter’s internal structure; (ii) In deriving Eq. (16), we have neglected order $\bar{\Omega}_s^2$ corrections to the mode frequency and the tidal overlap¹.

Figure 1 shows the dynamical corrections $\delta_{lm} \equiv \Delta k_{lm}/k_{lm}^{(hs)} = (k_{lm} - k_{lm}^{(hs)})/k_{lm}^{(hs)}$ to Jupiter’s tidal Love numbers as a function of the orbital frequency Ω_{orb} of the perturbing satellite. These results are obtained using the $n = 1$ isentropic model, which gives the hydrostatic values $k_{lm}^{(hs)} \simeq 0.550, 0.213, 0.219, 0.121, 0.123$ for $(lm) = (22), (31), (33), (42), (44)$, respectively. Although these hydrostatic values may not correspond to the “true” values for Jupiter because of the simplicity of the polytrope model and the $\bar{\Omega}_s^2$ corrections (see above), the dynamical corrections δ_{lm} shown in Fig. 1 are robust.

Our results depicted in Fig. 1 can be compared to those of Idini & Stevenson (2021) obtained using more complicated calculations (see their Table 2). Our δ_{22} , δ_{33} and δ_{44} values (evaluated for the orbital frequencies of Io, Europa, Ganymede and Callisto) agree reasonably well with theirs, but our δ_{31} , δ_{42} values are a factor of a few smaller.

Finally, using Table 1, we can easily check that the contributions from p-modes to k_{lm} are negligible.

4. INERTIAL-MODE CONTRIBUTION

In addition to f-modes and p-modes, a rotating planet possesses a spectrum of inertial modes supported by Coriolis force.

For $n = 1$ polytrope, the $m = 2$ inertial modes have been computed by Xu & Lai (2017) using a spectral code. The mode properties are

$$\omega_+ = 0.556\Omega_s, \quad \varepsilon_+ = 0.28\Omega_s, \quad \bar{Q}_+ = 0.015\bar{\Omega}_s^2 \quad (21)$$

¹ Both $\bar{\omega}_0^2$ and \bar{Q}_l^2 in Eq. (16) can have corrections of order $\bar{\Omega}_s^2$. These corrections do not affect $\Delta k_2/k_2^{(\text{hs})}$ to the leading order. Note that for $n = 0$ (incompressible MacLaurin spheroid), the exact expressions for the mode frequency and tidal overlap coefficient are available [see Eq. (3.4) and Eq. (3.22) of Ho & Lai (1999)].

for the prograde mode, and

$$\omega_- = -1.10\Omega_s, \varepsilon_- = -0.55\Omega_s, \bar{Q}_- = 0.010\bar{\Omega}_s^2 \quad (22)$$

for the retrograde mode, where Q_\pm is the tidal coupling coefficient $Q_{\alpha,22}$. Since $\omega < 0$, we can write the inertial mode contribution of k_2 as

$$k_{2,\text{in}} = \frac{2\pi}{5} \left[\frac{\bar{Q}_+^2}{\bar{\varepsilon}_+(\bar{\omega}_+ + |\bar{\omega}|)} + \frac{\bar{Q}_-^2}{|\bar{\varepsilon}_-|(|\bar{\omega}_-| - |\bar{\omega}|)} \right]. \quad (23)$$

Define $\hat{\omega} \equiv \omega/\Omega_s$ (and similarly $\hat{\omega}_\pm$ and $\hat{\varepsilon}_\pm$) and $\hat{Q}_\pm \equiv Q_\pm/\bar{\Omega}_s^2$, we have

$$k_{2,\text{in}} = \frac{2\pi}{5} \bar{\Omega}_s^2 \left[\frac{\hat{Q}_+^2}{\hat{\varepsilon}_+(\hat{\omega}_+ + |\hat{\omega}|)} + \frac{\hat{Q}_-^2}{|\hat{\varepsilon}_-|(|\hat{\omega}_-| - |\hat{\omega}|)} \right]. \quad (24)$$

For $n = 1$ polytrope, this gives

$$k_{2,\text{in}} = \frac{2\pi}{5} \bar{\Omega}_s^2 \times 10^{-4} \left(\frac{8.04}{0.556 + |\hat{\omega}|} + \frac{1.82}{1.10 - |\hat{\omega}|} \right). \quad (25)$$

For Jupiter-Io system, $\hat{\omega} = 2\Omega_{\text{orb}}/\Omega_s - 2 = -1.53$, it is clear that $k_{2,\text{in}} \ll 1$. In general, unless $|\hat{\omega}|$ happens to be very close to $|\hat{\omega}_-|$ (to within 10^{-4}), the contribution of the inertial modes to the Love number is negligible.

5. STABLE STRATIFICATION AND G-MODE CONTRIBUTION

In Sections 3-4 we considered fully isentropic models for Jupiter, i.e., the adiabatic index $\Gamma_1 \equiv (\partial \ln P / \partial \ln \rho)_s$ equals the polytropic index $\Gamma \equiv d \ln P / d \ln \rho = 1 + 1/n$. In reality, some regions of the planet may be stably stratified, with $\Gamma_1 > \Gamma$. Indeed, the gravity measurement by *Juno* and structural modeling suggest that Jupiter could have a diluted core and a total heavy-element mass of 10-24 Earth masses, with the heavy elements distributed within an extended region covering nearly half of Jupiter's radius (Wahl et al. 2017; Debras & Chabrier 2019; Stevenson 2020). The composition gradient would provide stable stratification, and the planet would then possess g-modes.

To explore of how g-modes influence the tidal love numbers, we consider three simple planetary models, all having a $n = 1$ density profile ($\Gamma = 2$), but with different adiabatic index profiles: (i) $\Gamma_1 = 2.4$ throughout the planet; (ii) $\Gamma_1 = 2.1$ throughout the planet; (iii) Stable stratification only for $r \lesssim 0.5R$, with

$$\Gamma_1(r) = 2 + \frac{0.4}{1 + \exp[(r - 0.5R)/(0.05R)]}. \quad (26)$$

For each model, we compute the f-modes and g-modes of a nonrotating planet (see Table 1), and use Eqs. (12)-(13) to account for the effect of rotation on the modes.

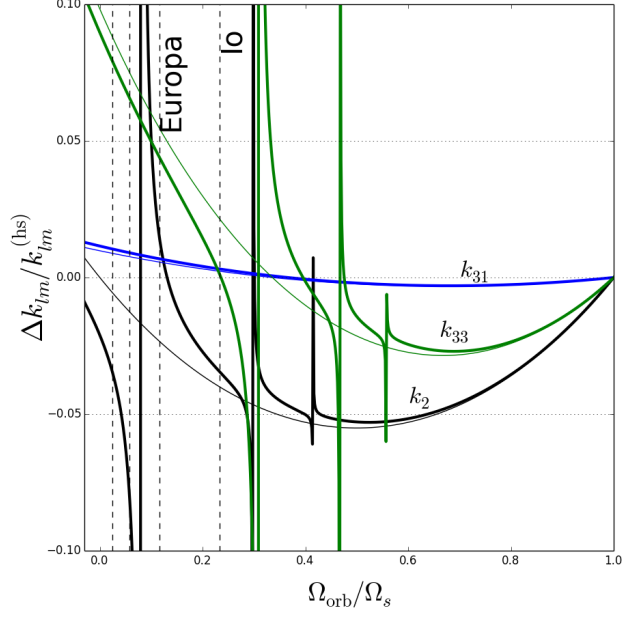


Figure 2. Same as Fig. 1, but for the $n = 1$, $\Gamma_1 = 2.4$ planetary model, which possesses g-modes. The heavy solid curves include the contributions of f-modes and first three radial-order g-modes to k_{lm} , the light solid curves include only f-modes (for the $n = 1$ isentropic model, as in Fig. 1).

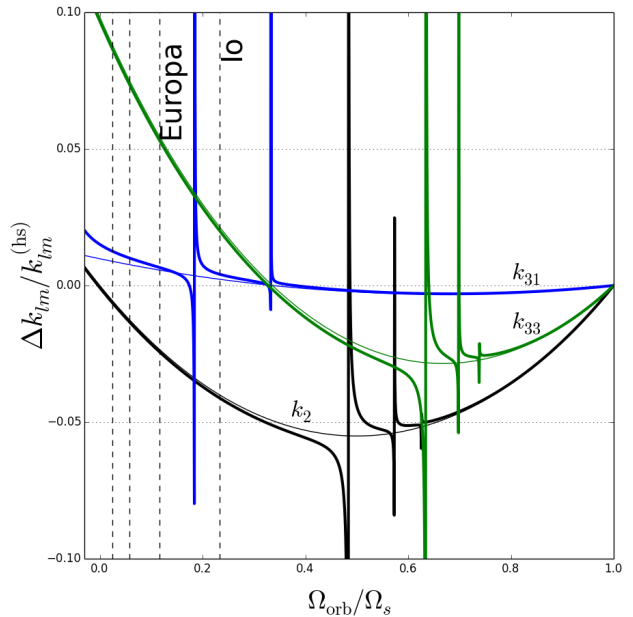


Figure 3. Same as Fig. 2, but for the $n = 1$, $\Gamma_1 = 2.1$ planetary model.

We include only the first three radial-order g-modes in our calculation of k_{lm} . The perturbative approach of the

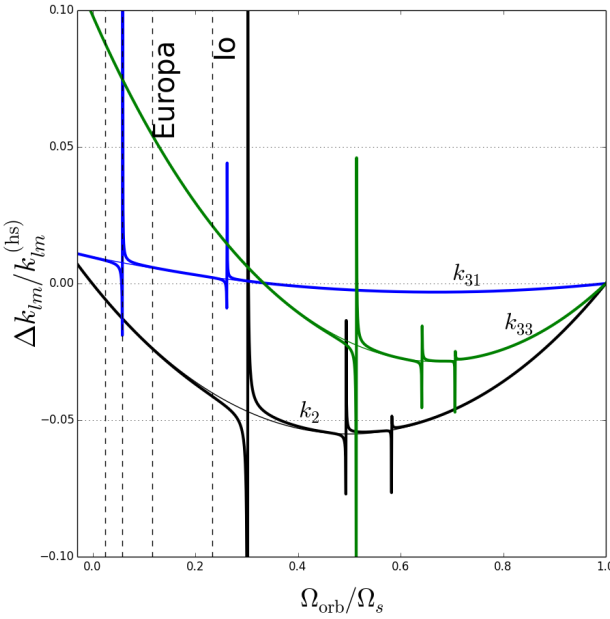


Figure 4. Same as Fig. 2, but for the $n = 1$ model with stable stratification concentrated in the $r \lesssim 0.5R$ region (see Eq. 26).

rotational effect is approximately valid for these modes since $mC\Omega_s$ is much less than the mode frequency $|\omega_0|$.

Figures 2-4 show the results for the dynamical Love numbers based on the three models. It is obvious that significant dynamical correction to the hydrostatic $k_{lm}^{(hs)}$ occurs around the resonance, where $\omega_\alpha = \omega$. The “strength” of each resonance is measured by the tidal overlap coefficient, and a large $|Q_l|$ value implies that the “width” of the resonant feature is larger (see Eq. 16). For the $\Gamma_1 = 2.4$ model, the stratification is strong, the broad/strong resonance with the g_1 mode can affect k_{lm} associated with the Galilean moons (Fig. 2). For the $\Gamma_1 = 2.1$ model, the resonance feature is much

weaker/narrower because of the weaker stratification (Fig. 3). For the model with stratification concentrated in the core [model (iii)], the $|Q_l|$ values are significantly reduced, and the resonance width is also diminished (Fig. 4).

Note that Figures 2-4 do not include contributions from high-order g-modes. These modes (with mode frequencies comparable to Ω_s) become mixed with inertial modes (so-called “inertial-gravity” modes; see Xu & Lai 2017) and cannot be treated using Eqs. (12)-(13). However, because of their small tidal overlap coefficients, they are unlikely to be important contributors to k_{lm} except for the coincidence of an extremely close resonance.

6. CONCLUSION

We have derived a general equation (Eq. 11) for computing the dynamical Love number k_{lm} of a rotating giant planet in response to the tidal forcings from its satellites. In most situations, the Love number is dominated by the tidal response of f-modes, and the general expression reduces to Eq. (16), which can be easily evaluated using the mode properties of nonrotating planet models (see Table 1). We show that the 4% discrepancy between the measured k_2 of Jupiter and the theoretical hydrostatic value can be naturally explained by the dynamical response of Jupiter’s f-modes to the tidal forcing from Io – the key is to include the rotational (Coriolis) effect in the tidal response in a self-consistent way. We also show that the contributions of the inertial modes to the Love number k_2 are negligible.

We have also explored the effect of stable stratification in Jupiter’s interior on the Love numbers. If sufficiently strong stratification exists in a large region of the planet’s interior, g-mode resonances may influence the dynamical Love numbers associated with the tidal forcing from the Galilean moons. Thus, precise measurements of various k_{lm} could provide constraints on the planet’s interior stratification.

REFERENCES

Debras, F., & Chabrier, G. 2019, *Astrophys. J.* 872, 100
 Durante, D., et al. 2020, *Geophysical Research Letters*, 47, e2019GL086572
 Friedman, J.L., & Schutz, B.F. 1978, *Astrophys. J.* 221, 937
 Ho, W.C.G., & Lai, D. 1999, *MNRAS*, 308, 153
 Idini, B., & Stevenson, D.J. 2021, *PSJ*, in press (arXiv:2102.09072)
 Lai D., & Wu, Y. 2006, *Phys. Rev. D* 74, 024007
 Schenk, A.K. et al. 2002, *Phys. Rev. D* 65, 024001
 Stevenson, D.J. 2020, *AREP*, 48, 465
 Unno, W., et al. 1989, *Nonradial oscillations of stars*, University of Tokyo Press
 Wahl, S. M., et al. 2017, *Geophys. Res. Lett.* 44, 4649
 Wahl, S. M., Parisi, M., Folkner, W. M., Hubbard, W. B., & Militzer, B. 2020, *The Astrophysical Journal*, 891, 42
 Xu, Wenrui, & Lai, D. 2017, *Phys. Rev. D* 96, 083005